

# Search for CP violation in tau decays.

Y. Maravin<sup>a \*</sup>

<sup>a</sup>Physics Department, Southern Methodist University, Dallas, TX 75275-0175, USA  
E-mail: maravin@mail.physics.smu.edu

The results of the searches for CP non-conservation in the decays of  $\tau$  leptons are presented. No evidence of violation of CP symmetry is observed neither in CLEO nor in BELLE data. Interpretation of these results is done within the framework of a model with a scalar boson exchange. Limits on the imaginary part of the coupling constant  $\Lambda$ , parameterizing the relative contribution of diagrams that would lead to CP violation, are  $-0.046 < \Im(\Lambda) < 0.022$  at 90% C.L. and  $|\Im(\Lambda)| < 1.7$  at 90% C.L. in  $\tau \rightarrow \pi\pi^0\nu_\tau$  and  $\tau \rightarrow K\pi^0\nu_\tau$  modes, respectively.

## 1 Introduction

The violation of the combined symmetry of charge conjugation and parity (CP) has been of long-standing interest as a possible source of the matter-antimatter asymmetry [1] in the Universe. Efforts to search for the CP-violating effects have concentrated so far on the hadronic sector. CP violation in strange meson decay has been the subject of intensive investigation since its first observation [2] in 1964. Studies of hadronic [3] as well as semileptonic [4, 5, 6] kaon decays provide precision measurements of the CP violation parameters. Searches for corresponding asymmetries in  $B$  meson decays are the focus of several large ongoing experiments [7, 8]. Recent indications of possible neutrino oscillations [9] make it important to re-examine the question of CP non-conservation in the leptonic sector. Such violation is forbidden in the Standard Model but appears as a consequence of its various extensions [10]. Among best-known theoretically are the multi-Higgs-doublet models (MHDM) [11, 12, 13]. Models predicting lepton flavor violation often also predict CP violation in lepton decays [14, 15]. Precision studies of muon decay parameters [16, 17] show no indication for CP violation in such decay.

In this talk I discuss three searches for CP violation in tau lepton decays. The searches for the CP-violating asymmetry in single tau decays were done by the CLEO [18] and the BELLE [19] collaborations. In the third analysis by CLEO [20] correlated tau decays are used to search for a non-zero value of CP-odd optimal observable indicating CP violation.

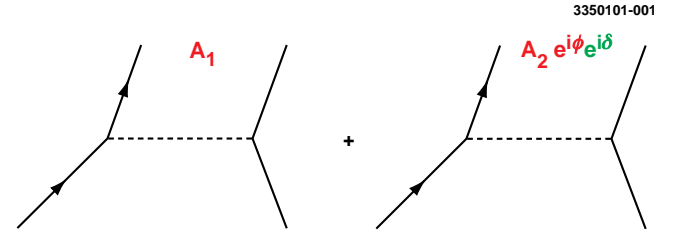


Figure 1: Interference between two amplitudes with CP-even and CP-odd relative phases  $\delta$  and  $\phi$ .

## 2 CP violation

CP violation is the observable difference between a process ( $a \rightarrow b$ ) and its CP conjugate ( $\bar{a} \rightarrow \bar{b}$ ). The necessary condition to observe such a difference is to have a non-zero CP violating phase  $\phi$  in the Lagrangian describing the process. Since the absolute value of a CP-odd phase does not have a physical meaning, CP violation can be observed only when interfered with a CP-even phase  $\delta$ . Therefore, two interfering diagrams is needed to observe CP violation (see Fig. 1). The probability density for such a process is given by:

$$|\mathcal{A}|^2 = (A_1 + A_2 e^{i\phi} e^{i\delta})(A_1 + A_2 e^{-i\phi} e^{-i\delta})$$

$$= A_1^2 + A_2^2 + 2A_1 A_2 \cos \phi \cos \delta - \underline{2A_1 A_2 \sin \phi \sin \delta}. \quad (1)$$

The last, underlined, term is CP-odd since the phase  $\phi$  changes sign under CP conjugation. If this term is not equal to zero, physical observables between a process ( $a \rightarrow b$ ) and its CP conjugate ( $\bar{a} \rightarrow \bar{b}$ ) may be different and CP is violated.

$A_1$  and  $A_2$  denote the amplitudes and for physical processes they must be different from zero. Thus CP-

\*Talk given at the Frontiers in Contemporary Physics-II (FCP01) Workshop, Vanderbilt University, Nashville TN, 5-10 March 2001.

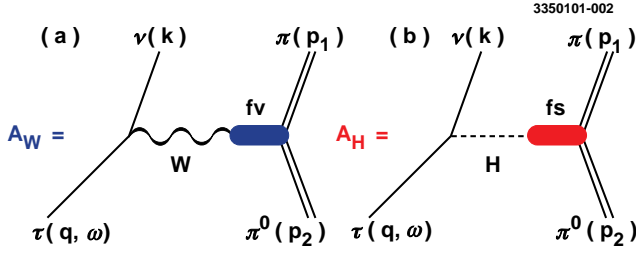


Figure 2: Amplitude for (a) standard W exchange, (b) scalar exchange for  $\tau \rightarrow \pi\pi^0\nu_\tau$  decay.

odd term is not equal to zero if the factors  $e^{i\phi}$  and  $e^{i\delta}$  differ from zero and are complex.

### 3 CP violation in $\tau$ decays

A possible scenario for CP violation in  $\tau$  lepton decays is described [11] by the interference of the Standard Model decay amplitude mediated by the W boson (amplitude  $A_W$ ) with the amplitude mediated by the charged Higgs boson in the multi-Higgs-doublet model (amplitude  $A_H$ ). These amplitudes play the roles of  $A_1$  and  $A_2$  of the previous section (see Fig. 2). In this scenario, the charged Higgs couples to quarks and leptons with complex coupling constants and, thus, there can be a weak complex (CP-violating) phase ( $\sin \phi \neq 0$ ). The overall Higgs coupling to the  $\pi\pi^0$  system is denoted by  $\Lambda$ :

$$\Lambda = \Re(\Lambda) + i\Im(\Lambda) = |\Lambda|(\cos \phi + i \sin \phi). \quad (2)$$

The usual choice for the CP-even phase  $\delta$  is a strong phase [21] which arises due to the QCD final state interactions between quarks. In the following, I consider only  $\tau$  decays into hadronic final states and a neutrino. There are several possible tau decay modes that can be used to search for CP violation. The  $\tau \rightarrow K\pi\nu_\tau$  mode is favored with the largest possible CP violation effects [18]. The corresponding branching fraction is, however, Cabbibo suppressed and the kaon identification efficiency in CLEO data is small, thus, leading to a small sample that can be used for experimental studies. This is not the case for  $\tau \rightarrow \pi\pi^0\nu_\tau$  decay due to the largest branching fraction of tau decaying into two pion state. However, scalar decaying into two pions implies isospin violation [22]. Therefore, the CP violating effects in this mode are suppressed.<sup>†</sup> In the following I discuss searches for CP violation in both tau decay modes.

<sup>†</sup>The suppression factor is proportional to the mass difference of  $u$  and  $d$  quarks. It is estimated to be of the order of 0.0035 [22].

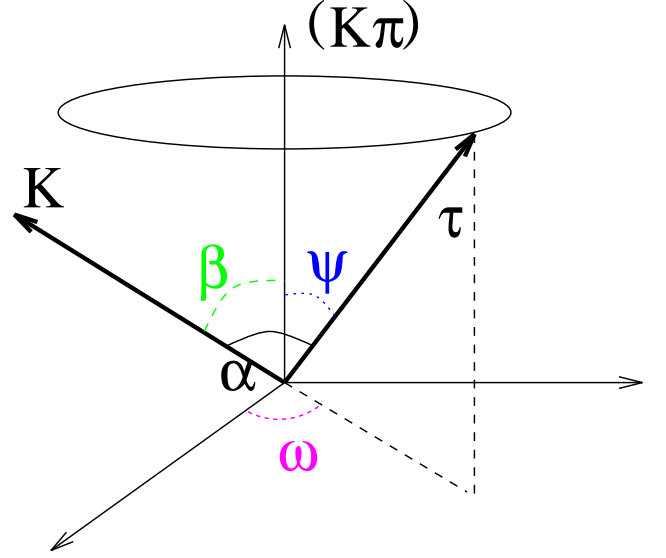


Figure 3: Definition of angles in the hadronic rest frame.  $(K\pi)$  defines the direction of the hadronic rest frame from the laboratory frame.

### 4 Searches for CP violation in single tau decays

There are two analyses [18, 19] which use single tau decays into  $K\pi\nu_\tau$  and  $\pi\pi^0$  final state using the technique proposed by J.H. Kühn and E. Mirkes [23, 22]. It can be shown that for the decays of unpolarized tau leptons the CP-odd part of the probability density is proportional to:

$$P_{odd} \sim \Im(\Lambda)\Im(e^{i\delta}) \cos \beta \cos \psi, \quad (3)$$

where  $\Im(\Lambda)$  is an imaginary part of the overall Higgs coupling (see Eq. 2),  $\delta$  is a relative strong phase between  $W$  and Higgs exchange diagrams.  $\beta$  and  $\psi$  are angles between a hadron,  $\tau$  lepton and direction of the hadronic rest frame in the laboratory frame (see Fig. 3). Therefore, the distributions of  $\cos \beta \cos \psi$  for  $\tau^+$  and  $\tau^-$  decays are given by:

$$\frac{dN(\tau^+)}{d \cos \beta \cos \psi} = \text{const} + c_1 \Im(\Lambda) \cos \beta \cos \psi, \quad (4)$$

and

$$\frac{dN(\tau^-)}{d \cos \beta \cos \psi} = \text{const} + c_1 \Im(\Lambda^*) \cos \beta \cos \psi, \quad (5)$$

where  $\text{const}$  is contribution from the standard, CP-even part of the probability density and  $c_1$  is a proportionality constant. Asymmetry, defined as a difference between Eqs. 4 and 5 normalized by the sum of these distributions is:

$$A_{cp} = \frac{c_1}{\text{const}} \Im(\Lambda) \cos \beta \cos \psi. \quad (6)$$

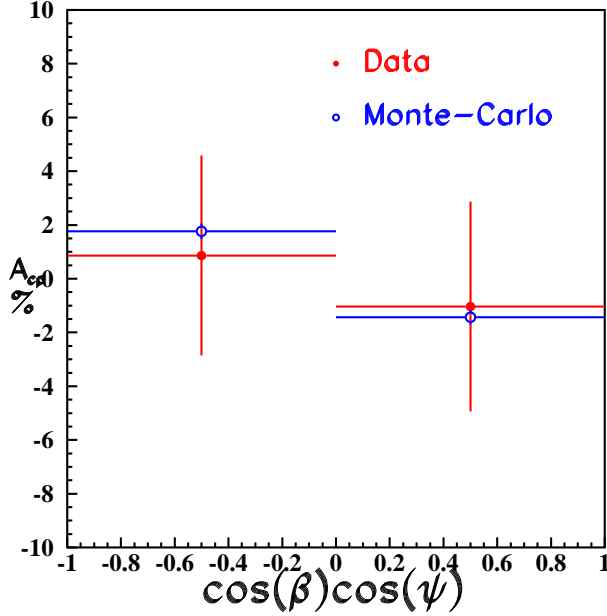


Figure 4: Asymmetry  $A_{cp}$  as a function of  $\cos \beta \cos \psi$  (CLEO).

Non-zero slope in  $\cos \beta \cos \psi$  distribution indicates CP violation. The value of  $\Im(\Lambda)$  can be determined if empirical coefficient  $c_1/\text{const}$  is known.<sup>‡</sup>

#### 4.1 CLEO $\tau \rightarrow K\pi\nu_\tau$ results

The first search for CP violation in tau decays is performed in the  $\tau \rightarrow K\pi\nu_\tau$  mode [18]. Data collected from  $e^+e^-$  collisions at a center of mass energy ( $\sqrt{s}$ ) of 10.6 GeV with the CLEO II detector [24] at the Cornell Electron Storage Ring (CESR) is used in this analysis. The total integrated luminosity of the data sample is  $4.8 \text{ fb}^{-1}$ , corresponding to the production of  $4.4 \times 10^6$  tau pairs. A  $\tau^- \rightarrow K_s^0 h^- \nu_\tau$ ,  $K_s^0 \rightarrow \pi^- \pi^+$  event sample is selected since three charged tracks in the final state are well measured. Here  $h^-$  is a charged pion or kaon. The standard selection criteria is used to reconstruct  $\tau \rightarrow K_s^0 h \nu_\tau$  by CLEO in previous analysis [25].

Observed asymmetry  $A_{cp}$  (see Eq. 6) in the data sample for the positive and for the negative values of  $\cos \beta \cos \psi$  after subtraction of the background is given in Table 1. The distribution of  $A_{cp}$  for the data and Standard Model Monte Carlo is illustrated in Fig. 4.

To relate the observed asymmetry  $A_{cp}$  to the imaginary part of the coupling constant  $\Lambda$ , the value of the proportionality coefficient  $c_1$  (see Eq. 6) is estimated using modified TAUOLA package [26]. No CP violation is

<sup>‡</sup>Can be estimated in Monte Carlo simulation.

Table 1: Asymmetry  $A_{cp}$  for negative and positive values of  $\cos \beta \cos \psi$ , CLEO Collaboration.

$\cos \beta \cos \psi$	$A_{cp}$
$\cos \beta \cos \psi < 0$	$0.009 \pm 0.038$
$\cos \beta \cos \psi > 0$	$-0.010 \pm 0.039$

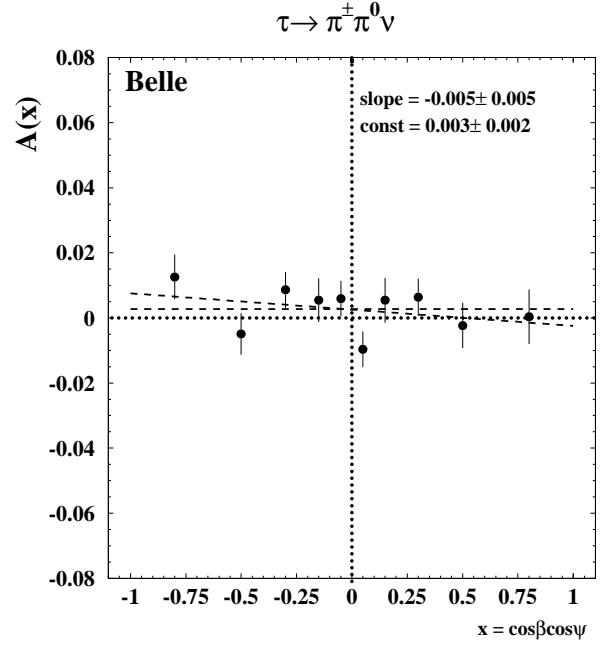


Figure 5: Asymmetry  $A_{cp}$  as a function of  $\cos \beta \cos \psi$ . The dashed lines are fits with a straight line or a constant (Belle).

observed and the following upper limit on CP-violation is set:

$$|\Im(\Lambda)| < 1.7, \text{ at } 90\% \text{ C.L.} \quad (7)$$

#### 4.2 BELLE $\tau \rightarrow \pi\pi^0\nu_\tau$ results

There is an ongoing search [19] by the BELLE Collaboration for CP violation in  $\tau \rightarrow \pi\pi^0\nu_\tau$  mode using the same technique. The data sample used in this analysis has been collected in  $e^-e^+$  collisions at a center of mass energy of 10.6 GeV with the Belle detector at the KEK asymmetric energy collider (KEKB) [27]. The total integrated luminosity accumulated during this period is  $6.7 \text{ fb}^{-1}$ , corresponding to 6.2 million tau pairs. The final sample of  $\tau \rightarrow \pi\pi^0\nu_\tau$  contains  $2.6 \times 10^5$  events. Using this sample the asymmetry from  $\tau^+$  and  $\tau^-$  decays has been measured in two intervals of  $\cos \beta \cos \psi$  similarly to the previous section. The values of the observed asymmetry are given in Table 2. The distribution of the asymmetry

Table 2: Asymmetry  $A_{cp}$  for negative and positive values of  $\cos \beta \cos \psi$ , Belle collaboration.

$\cos \beta \cos \psi$	$A_{cp}$
$\cos \beta \cos \psi < 0$	$0.0056 \pm 0.0027$
$\cos \beta \cos \psi > 0$	$-0.0004 \pm 0.0027$

is illustrated in Fig. 5. The value of the asymmetry is consistent with previous CLEO result and indicates no CP violation in  $\tau \rightarrow \pi\pi^0\nu_\tau$  decays within measurement errors:

$$|A_{cp}| < 0.010, \text{ at } 90 \% \text{ C.L.} \quad (8)$$

The limit on the imaginary part of the scalar coupling will be set in the near future.

#### 4.3 Summary of searches in single tau decays

The first search for CP violation in  $\tau$  decays is done in  $\tau \rightarrow K\pi\nu_\tau$  mode and provides for the first time a restriction on the imaginary part of a scalar coupling in tau decays:

$$|\Im(\Lambda)| < 1.7, \text{ at } 90\% \text{ C.L.} \quad (9)$$

Analysis using a single tau decaying into  $\pi\pi^0\nu_\tau$  final state is in progress and current upper limit on the CP-violating asymmetry is:

$$|A_{cp}| < 0.010, \text{ at } 90 \% \text{ C.L.} \quad (10)$$

This limit will be improved with better understanding of the systematics and an increase of the data sample. A conversion of the above upper limit to the imaginary part of the scalar coupling will be done in the near future.

Searches for CP violation in a single  $\tau$  decay are sensitive only to a spin-independent CP-violating term in the decay rate. Other spin-dependent terms are proportional to tau polarization vector and, therefore, average to zero. However, the situation is different for decays of tau pairs produced in  $e^+e^-$  annihilations, where the parent virtual photon introduces correlations of the  $\tau^+$  and  $\tau^-$  spins. This correlation provides an additional constraint which permits to be sensitive to all CP-odd terms of the decay rate and maximizes the sensitivity to possible CP-violating effects. In the following, I discuss an analysis [20] without these disadvantages.

## 5 CP violation in correlated tau decays

To maximize the sensitivity of our search an optimal variable is constructed, first proposed [28] by D. Atwood and A. Soni,  $\xi$ , with the smallest associated statistical error.

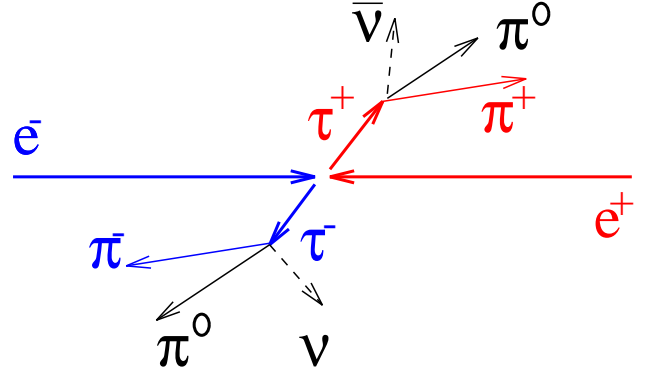


Figure 6: Correlated decay of tau pair into  $\pi\pi^0\nu_\tau$  each.

The variable is equal to the ratio of the CP-odd and CP-even parts of the total cross section assuming that the absolute value of the coupling  $\Lambda$  is unity:

$$\xi = \frac{P_{odd}}{P_{even}}, \quad (11)$$

where  $P_{odd}$  and  $P_{even}$  are the CP-odd and CP-even parts of the total cross section. These terms are functions of the vector and scalar hadronic currents. A vector hadronic current is parameterized by the relative momentum between the charged and neutral pions multiplied by the vector form factor,  $f_v$ , described by  $\rho$  Breit-Wigner shape:

$$f_v = \frac{-m^2}{s - m^2 + im\Gamma(s)}, \quad (12)$$

where  $s$  is a squared invariant mass of two pions,  $m_\pi$  is a pion mass, and  $m$  and  $\Gamma(s)$  are the mass and the momentum-dependent width of the resonance, respectively. The latter is defined as:

$$\Gamma(s) = \begin{cases} \frac{m}{\sqrt{s}} \left( \frac{s - 4m_\pi^2}{m^2 - 4m_\pi^2} \right)^{3/2} & \text{if } s > (2m_\pi)^2 \\ 0 & \text{elsewhere.} \end{cases} \quad (13)$$

Here, the contribution from the  $\rho'$  resonance [29] is neglected. The scalar hadronic current is parameterized as a product of a dimensional quantity,  $M = 1 \text{ GeV}/c^2$  providing overall normalization, and a scalar form factor  $f_s$ . The choice of the scalar form factor is not unambiguous. Three possible cases are studied: one with  $f_s = 1$ , the second with  $f_s$  described by the  $a_0(980)$  Breit-Wigner shape, and the third with  $f_s$  described by  $a_0(1450)$  Breit-Wigner shape (see Eq. 12) with a width given by:

$$\Gamma(s) = \begin{cases} \frac{m}{\sqrt{s}} \left( \frac{s - 4m_\pi^2}{m^2 - 4m_\pi^2} \right)^{1/2} & \text{if } s > (2m_\pi)^2 \\ 0 & \text{elsewhere.} \end{cases} \quad (14)$$

Since  $P_{odd}$  is proportional to the imaginary part of  $\Lambda$ , then it can be expressed as:

$$P_{odd}(\Lambda) = \Im(\Lambda)P_{odd}(1), \quad (15)$$

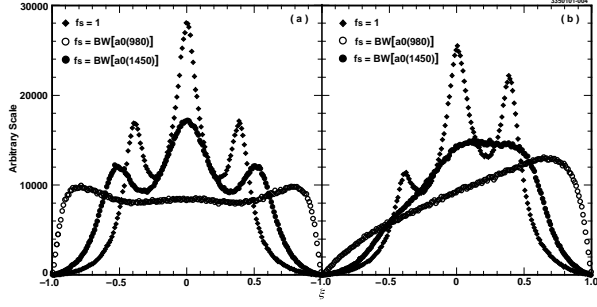


Figure 7: Optimal observable  $\xi$  for (a) Monte Carlo with no CP violation and (b) Monte Carlo with a maximal CP violation  $\Im(\Lambda) = 1$ .

and

$$\langle \xi \rangle = \Im(\Lambda) \int \frac{P_{\text{odd}}(1)^2}{P_{\text{even}}} dLips. \quad (16)$$

The integral in Eq. 16 is always larger than or equal to zero, and equality occurs only if the odd part of the cross section vanishes. Therefore, the average value of  $\xi$  is proportional to the imaginary part of the Higgs coupling constant and is positive if  $\Im(\Lambda) > 0$  and negative if  $\Im(\Lambda) < 0$ . Monte Carlo simulation of the  $\xi$  distributions for the three choices of the scalar form factors and no CP violation are shown in Fig. 7(a). The same distributions for the CP violating case  $\Im(\Lambda) = 1$  are shown in Fig. 7(b). The structure in these distributions is due to the resonant structure in the vector and scalar form factors.

To relate the observed mean value of the optimal observable  $\langle \xi \rangle$  to the imaginary part of the coupling constant  $\Lambda$ , the  $\Im(\Lambda)$  dependence of  $\langle \xi \rangle$  must be known. To the first order the mean value is proportional to  $\Im(\Lambda)$  with a proportionality coefficient  $c$ :

$$\langle \xi \rangle = c \times \Im(\Lambda). \quad (17)$$

The value of this coefficient is estimated using Monte Carlo simulation as described in the Section 5.2.

### 5.1 Data and Monte Carlo Samples

The data used in this analysis were collected at the Cornell Electron Storage Ring (CESR) at or near the energy of the  $\Upsilon(4S)$ . The data correspond to a total integrated luminosity of  $13.3 \text{ fb}^{-1}$  and contain 12.2 million  $\tau^+\tau^-$  pairs. Versions of the CLEO detector employed here are described in Refs. [24, 30]. From this data sample, events consistent with  $e^+e^- \rightarrow \tau^+\tau^-$  interactions are selected where each  $\tau$  decays into the  $\pi\pi^0\nu_\tau$  final state. The event selection follows mostly the procedure developed originally for the study of the  $\tau \rightarrow \rho\nu_\tau$  decays [31]. In the following section it is shown that the event selection criteria do not introduce artificial CP-violating effects.

Table 3: Average values of the optimal observable  $\langle \xi \rangle$  for the Standard Model Monte Carlo and the proportionality coefficient  $c$  for the CP asymmetry fits for different scalar form factors.

Form factor, $f_s$	$\langle \xi \rangle, 10^{-3}$	$c, 10^{-3}$
1	$0.7 \pm 0.6$	$66.8 \pm 4.3$
$BW(a_0(980))$	$1.0 \pm 1.1$	$586.4 \pm 19.4$
$BW(a_0(1450))$	$0.5 \pm 0.8$	$145.8 \pm 7.3$

To estimate backgrounds large samples of Monte Carlo events are analyzed following the same procedures that are applied to the actual CLEO data. All non-tau backgrounds are found to be negligible. The main remaining background is due to the  $\tau$ -pair events in which one of the  $\tau$ 's decays into  $\rho\nu_\tau$  while the other decays into  $\pi^0\nu_\tau$  and the photons from one of the  $\pi^0$ 's are not detected. The contamination from this background source is estimated to be 5.2%. The second largest background contribution of 2.1% is due to one of the  $\tau$ 's decaying into the  $K^*\nu_\tau$  final state producing a neutral pion plus a charged kaon which is mistaken for a pion. All other tau decays provide much smaller contributions with the largest being less than 0.7%. The total background contamination from tau decays is estimated to be 9.9%. This background neither introduces a bias in the  $\langle \xi \rangle$  distribution nor modifies the value of the coefficient  $c$ , defined in Eq. 17.

### 5.2 Calibration

To relate the observed mean value of the optimal observable  $\langle \xi \rangle$  to the imaginary part of the coupling constant  $\Lambda$ , coefficient  $c$  must be determined. It is estimated using several signal Monte Carlo samples generated<sup>§</sup> with different values of  $\Im(\Lambda)$ . For each sample we calculate the average value of the optimal observable  $\xi$  and plot it as a function of  $\Im(\Lambda)$ . For each form of the scalar component, the calculated asymmetry distribution is fit to a straight line to obtain the calibration coefficients. To check that the selection criteria do not create an artificial asymmetry the mean value of the optimal observable is calculated for Standard Model Monte Carlo samples for each choice of the scalar form factor. These values along with calculated coefficients  $c$  are listed in Table 3. For all three form factors, the mean value of  $\xi$  for the Standard Model Monte Carlo sample is consistent with zero within its statistical error. Therefore, event selection criteria do not introduce an artificial asymmetry in the  $\xi$  distribution. The coefficients from Table 3 are used to calculate  $\Im(\Lambda)$ .

<sup>§</sup>These events are generated with full GEANT-based detector simulation [32] and pattern recognition software.

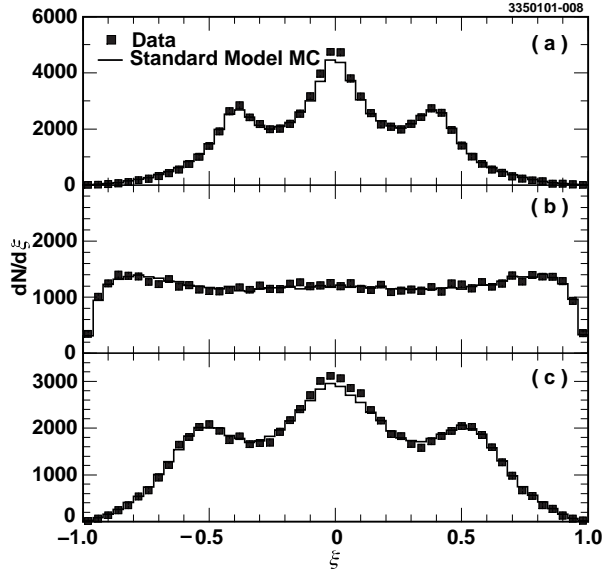


Figure 8: The distribution of the CP violation sensitive variable  $\xi$  for the data (dots) compared to the Standard Model Monte Carlo prediction (solid line) for (a)  $f_s=1$ , (b)  $f_s = BW(a_0(980))$  and (c)  $f_s = BW(a_0(1450))$ .

Table 4: Average value of the optimal observable  $\xi$  after subtracting the average value for Standard Model Monte Carlo, calculated value of  $\Im(\Lambda)$  and 90% C.L. intervals on  $\Im(\Lambda)$ .

$f_s$	$\langle \xi \rangle, 10^{-3}$	$\Im(\Lambda), 10^{-2}$	$\Im(\Lambda), 90\% \text{ C.L.}$
1	$-0.8 \pm 1.4$	$-1.2 \pm 2.1$	$(-0.046; 0.022)$
$a_0(980)$	$-0.6 \pm 2.4$	$-0.1 \pm 0.4$	$(-0.008; 0.006)$
$a_0(1450)$	$0.2 \pm 1.7$	$0.1 \pm 1.2$	$(-0.019; 0.021)$

### 5.3 Observed mean values

For each choice of the scalar form factor, a distribution in  $\xi$  is obtained. These distributions are shown in Fig. 8, with those from the Standard Model Monte Carlo simulations overlaid. From these distributions the mean values  $\langle \xi \rangle$  are computed after subtracting the average value for Standard Model Monte Carlo, which are reported in the first column of Table 4. In each case, the appropriate empirically-determined coefficient given in Table 3 is used to derive a value for the imaginary part of the Higgs coupling  $\Lambda$ , as described in the preceding section. These values along with the 90% confidence limits on  $\Im(\Lambda)$  are reported in the second and third columns of Table 4.

### 5.4 Summary

No sizable systematic errors are found<sup>¶</sup> which could alter the limits shown in Table 4. Within our experimental precision no significant asymmetry of the optimal variable is observed and, therefore, no CP violation in  $\tau$  decays. Due to the uncertainty in the choice of the scalar form factor the most conservative 90% confidence limits are used corresponding to  $f_s = 1$ :

$$-0.046 < \Im(\Lambda) < 0.022, \text{ at } 90\% \text{ C.L.}$$

These limits include the effects of possible systematic errors.

### 5.5 Pseudo-helicity method

In this section I discuss another method to search for CP violation in  $\tau$  decays. It is more intuitive but less sensitive than the optimal observable method described above.

The helicity angle,  $\theta_{\pi\pi}$ , is defined as the angle between the direction of the charged pion in the  $\pi\pi^0$  rest frame and the direction of the  $\pi\pi^0$  system in the  $\tau$  rest frame. In Standard Model, the helicity angle is expected to have a distribution corresponding to a vector exchange:

$$\frac{dN}{d \cos \theta_{\pi\pi}} \sim a + b \cos^2 \theta_{\pi\pi}. \quad (18)$$

For scalar-mediated decays, there is an additional term proportional to  $\cos \theta_{\pi\pi}$  that corresponds to the S-P wave interference and linearly proportional to the scalar coupling constant  $\Lambda$ . In general,  $\Lambda$  is complex and the term linear in  $\cos \theta_{\pi\pi}$  is proportional to the real and imaginary parts of the scalar coupling with coefficients  $c_1$  and  $c_2$ , respectively:

$$\frac{dN}{d \cos \theta_{\pi\pi}} \sim a + c_1 \Re(\Lambda) \cos \theta_{\pi\pi} + c_2 \Im(\Lambda) \cos \theta_{\pi\pi} + b \cos^2 \theta_{\pi\pi}. \quad (19)$$

The observation of the terms proportional to cosine of the helicity angle would indicate the scalar exchange in the tau decays.

In order to calculate the helicity angle tau rest frame must be known. Due to the unobserved neutrino, the tau rest frame can only be reconstructed with a two-fold ambiguity. Such ambiguity can be avoided by using the pseudo-helicity angle,  $\theta^*$ . This pseudo-helicity angle is obtained by replacing the tau rest frame with the laboratory rest frame where it is defined as an angle between the direction of  $\pi^\pm$  in the  $\pi\pi^0$  rest frame and the direction of the  $\pi\pi^0$  system in the lab frame. The difference between the pseudo-helicity distributions for the  $\tau^+$  and

<sup>¶</sup>The detailed description of the most significant effects is given elsewhere [20].

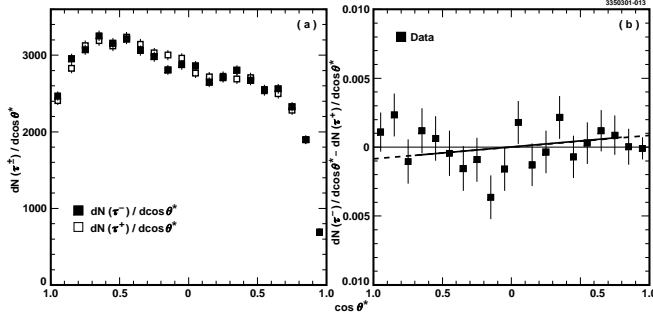


Figure 9: (a) Pseudo-helicity distribution for  $\tau^-$  and  $\tau^+$  in data, (b) difference between pseudo-helicity distributions for  $\tau^-$  and  $\tau^+$  in data. Solid line is a linear fit and dashed lines show extrapolation to the region excluded from the fit.

$\tau^-$  decays is expected to have the same form as given by Eq. 19 but with a different numerical coefficients.

The term including  $\Im(\Lambda)$  changes sign for tau leptons of opposite charges. Therefore, the difference of the pseudo-helicity distributions for positive and negative tau leptons has the term linear in  $\cos \theta^*$  proportional to the imaginary part of the scalar coupling  $\Lambda$  only:

$$\frac{dN(\tau^-)}{d \cos \theta^*} - \frac{dN(\tau^+)}{d \cos \theta^*} \sim 2c_2 \Im(\Lambda) \cos \theta^*. \quad (20)$$

The presence of this term indicates CP violation.

In this study, the same data sample is used as for the optimal observable analysis with the same selection criteria. The pseudo-helicity distribution for  $\tau^-$  and  $\tau^+$  is given in Fig. 9(a).

The structure in Fig. 9(a) is due to the variation in the efficiency as a function of charged pion momentum and  $\pi^0$  energy. To obtain the product of the imaginary part of the scalar coupling  $\Lambda$  and a linearity coefficient  $c_2$  (see Eq. 20), the difference of the two pseudo-helicity distributions for negative and positive tau leptons is fit to a first order polynomial. To minimize systematic effects due to soft pion reconstruction the fit is performed in the region of  $-0.7 < \cos \theta^* < 0.8$ , which corresponds to pions with momentum higher than 0.3 GeV/c. The obtained value of the slope for the data distribution is:

$$c_2 \Im(\Lambda) = (4.2 \pm 3.6) \times 10^{-4}$$

and illustrated in Fig. 9(b). It is consistent with zero within statistical error.

To determine the proportionality coefficient  $c_2$  the procedure described in Section 5.2 is followed. The slope of the difference of pseudo-helicity distributions is calculated after applying selection criteria. Five samples of 200,000 signal Monte Carlo events generated with different values of  $\Im(\Lambda)$  are used. Then, the calculated slope

dependence as a function of  $\Im(\Lambda)$  is fit to a straight line to obtain  $c_2$ :

$$c_2 = (107.5 \pm 12.6) \times 10^{-4}. \quad (21)$$

This coefficient is used to obtain the value of the imaginary part of the scalar coupling  $\Im(\Lambda)$  after the correction of the slope by Monte Carlo:

$$\Im(\Lambda) = 0.028 \pm 0.037, \quad (22)$$

and

$$-0.033 < \Im(\Lambda) < 0.089 \text{ at } 90\% \text{ C.L.} \quad (23)$$

As expected, the limit on the  $\Im(\Lambda)$  is less strict than the one obtained using the optimal observable.

## 6 Summary

I have discussed three searches for CP violation in the decays of tau leptons. No evidence for CP violation is observed within the experimental precision. First two analyses search for non-zero CP-violating asymmetry in the single tau decays to the  $K\pi\nu_\tau$  and  $\pi\pi^0\nu_\tau$  final states. The following upper limit on the imaginary part of the MHDm scalar coupling constant  $\Lambda$  is set in  $\tau \rightarrow K\pi\nu_\tau$  decays:

$$|\Im(\Lambda)| < 1.7 \text{ at } 90\% \text{ C.L.}, \quad (24)$$

The value of the asymmetry for  $\tau \rightarrow \pi\pi^0\nu_\tau$  is:

$$|A_{cp}| < 0.010, \text{ at } 90\% \text{ C.L.} \quad (25)$$

The conversion of this asymmetry to the value of  $\Im(\Lambda)$  will be done in the near future.

The third analysis used optimal variable to search for CP violation in correlated tau decays decaying into  $\pi\pi^0\nu_\tau$  final state each. The following confidence limits on  $\Im(\Lambda)$  are set:

$$-0.046 < \Im(\Lambda) < 0.022 \text{ at } 90\% \text{ C.L.} \quad (26)$$

All these results agree with each other and the limits on imaginary part of the coupling constant  $\Lambda$  restrict the size of the contribution of multi-Higgs-doublet model diagrams to the  $\tau$  lepton decay.

## References

1. A.D. Sakharov, ZhETF Pis. Red. **5**, 32 (1967); JETP Lett. **5**, 24 (1967).
2. J.H. Christenson, J.W. Cronin, V.L. Fitch and R. Turlay, Phys. Rev. Lett. **13**, 138 (1964).
3. NA48 Collaboration, V. Fanti *et al.*, Phys. Rev. B **465**, 335 (1999); KTeV Collaboration, A. Alavi-Harati *et al.*, Phys. Rev. Lett **83**, 22 (1999).



4. KEK-E246 Collaboration, M. Abe *et al.*, Phys. Rev. Lett. **83**, 4253 (1999).
5. S.R. Blatt *et al.*, Phys. Rev. D **27**, 1056 (1983).
6. I.I. Bigi and A.I. Sanda, *CP Violation*, (Cambridge University Press 1999).
7. B. Aubert *et al.* Phys. Rev. Lett. **86**, 2515 (2001).
8. A. Abashian *et al.* Phys. Rev. Lett. **86**, 2509 (2001).
9. Kamiokande Collaboration, T. Kajita *et al.*, Nucl. Phys. Proc. Suppl. **77**, 123 (1999).
10. M.B. Einhorn, J. Wudka, hep-ph/0007285.
11. Y. Grossman, Nucl. Phys. **B426**, 355 (1994).
12. Y. Grossman, Y. Nir, R. Rattazzi, SLAC-PUB-7379, hep-ph 9701231.
13. C.H. Albright, J. Smith, S.H.H. Tye, Phys. Rev. D **21**, 711 (1980).
14. K. Matsuda, N. Takeda, T. Fukuyama, H. Nishiura, Phys. Rev. D **62** 093001 (2000).
15. R. Kitano and Y. Okada, hep-ph/0012040.
16. H. Burkhardt *et al.*, Phys. Lett. B **160**, 343, (1985).
17. D.M. Kaplan, Phys. Rev. D **57**, 3827 (1998), and references therein.
18. CLEO Collaboration, S. Anderson *et al.*, Phys. Rev. Lett. **81**, 3823, (1998).
19. BELLE Collaboration, *Search for CP violation in  $\tau$  semi-leptonic decay  $\tau^\pm \rightarrow \pi^\pm \pi^0 \nu_\tau$* , Proc. ICHEP 2000, Osaka (2000).
20. CLEO Collaboration, P. Avery *et al.*, hep-ex/0104009; CLNS 01/1730, CLEO 01-6.
21. Y.S. Tsai, Phys. Rev. D **51**, 3172, (1995).
22. Y.S. Tsai, Nucl. Phys. Proc. Suppl. **55C**, 293 (1997).
23. J.H. Kuhn, E. Mirkes, Phys. Lett. B **398**, 407 (1997).
24. CLEO Collaboration, Y. Kubota *et al.*, Nucl. Instr. and Meth. **A320**, 66 (1992).
25. CLEO Collaboration, T. Coan, *et al.*, Phys. Rev. D **13**, 771 (1976).
26. KORALB (v. 2.2)/TAUOLA (v. 2.4): S. Jadach, J.H. Kuhn and Z. Was, Comput. Phys. Commun. **36**, 191 (1985) and *ibid* **64**, 275 (1991), *ibid* **76**, 361 (1993). Implementation of the scalar in  $\tau \rightarrow \pi\pi^0\nu_\tau$  decay is done by A. Weinstein and M. Schmidtler and can be obtained directly from them (ajw@caltech.edu).
27. B-Factory Design Report, KEK Report 95-7 (1995); K. Akai *et al.*, proc. 1999 particle Accelerator Conference, New York (1999); Y. Funakoshi *et al.*, Proc. 2000 European Particle Accelerator Conference, Vienna (2000).
28. D. Atwood and A. Soni, Phys. Rev. D **45**, 2405 (1992).
29. CLEO Collaboration, S. Anderson *et al.*, Phys. Rev. D **61**, 112002, (2000).
30. CLEO Collaboration, T.S. Hill, Nucl. Instr. and Meth. **A418**, 32 (1998).
31. CLEO Collaboration, M. Artuso *et al.*, Phys. Rev. Lett. **73**, 3762 (1994).
32. R. Brun *et al.*, GEANT 3.15, CERN DD/EE/84-1.